# Magnetism of finite graphene samples: Mean-field theory compared with exact diagonalization and quantum Monte Carlo simulations

Hélène Feldner,[1] Zi Yang Meng,[2] Andreas Honecker,[3] Daniel Cabra,[1] Stefan Wessel,[2] and Fakher F. Assaad[4]
[1]*Institut de Physique et Chimie des Matériaux de Strasbourg, UMR7504, CNRS-UdS, 23 rue du Loess, BP43, 67034 Strasbourg Cedex 2, France*
[2]*Institut für Theoretische Physik, Universität Stuttgart, 70550 Stuttgart, Germany*
[3]*Institut für Theoretische Physik, Georg-August-Universität Göttingen, Friedrich-Hund-Platz 1, 37077 Göttingen, Germany*
[4]*Institut für Theoretische Physik und Astrophysik, Universität Würzburg, Am Hubland, 97074 Würzburg, Germany*
(Received 28 October 2009; revised manuscript received 15 January 2010; published 11 March 2010)

The magnetic properties of graphene on finite geometries are studied using a self-consistent mean-field theory of the Hubbard model. This approach is known to predict ferromagnetic edge states close to the zigzag edges in single-layer graphene quantum dots and nanoribbons. In order to assess the accuracy of this method, we perform complementary exact diagonalization and quantum Monte Carlo simulations. We observe good quantitative agreement for all quantities investigated provided that the Coulomb interaction is not too strong.

DOI: 10.1103/PhysRevB.81.115416 PACS number(s): 71.10.Fd, 81.05.U−, 75.40.Mg

## I. INTRODUCTION

Graphene consists of a single layer of carbon atoms arranged in a honeycomb crystal lattice[1] and is a promising material with unique electronic properties. Among the most important characteristics, one should mention the presence of massless carriers, weak spin-orbit coupling, insensitivity to an external electrostatic potential (Klein paradox), fractional quantum Hall effect, etc. (for a review of the main features of graphene see Ref. 2). The electronic properties of graphene nanostructures such as nanoribbons or quantum dots are expected to be very different from bulk graphene. In fact, the Coulomb interaction is considerably enhanced in smaller geometries such as quantum dots, leading for example to unusual blockade effects.[3–5] On the other hand, the edge effect, which depends strongly on the geometry of the sample boundary, modifies the electronic structure of graphene.[6–8] In particular, it has been predicted that finite graphene samples can exhibit magnetic edge states (see, e.g., Refs. 9–19) suggesting potential spintronics applications of graphene nanodevices.[20]

It is common practice to use a mean-field theory (MFT) of the Hubbard model to investigate the magnetic properties of graphene in finite geometries (see, e.g., Refs. 9, 10, and 13–19). Such a MFT is applicable to any interaction and any geometry in a quite economic way: within the self-consistent mean-field (MF) approximation the main numerical effort is to solve the *single-electron* problem on a finite lattice. However, as far as we are aware, very little is known about the accuracy of this approximation.

The main purpose of the present paper is to address this issue and check the accuracy of the MFT. We start by recalling a real-space formulation of the MFT in Sec. II. In Sec. III we briefly look at periodic boundary conditions[21] and show that we can reproduce edge-ferromagnetism for a dot with zigzag edges.[14,15,19] The accuracy of the MFT is carefully examined in Sec. IV where we present a comparison with exact diagonalization for a small "dot" and quantum Monte Carlo (QMC) simulations on a larger system with periodic boundary conditions. We conclude with a summary and perspectives in Sec. V.

## II. MODEL AND COMPUTATION

Since we are interested in the magnetic properties of graphene, interactions should be taken into account. To this end, we study the Hubbard model whose Hamiltonian reads

$$H = -t \sum_{\langle i,j\rangle,\sigma} c^{\dagger}_{i,\sigma} c_{j,\sigma} + U \sum_{i} n_{i,\uparrow} n_{i,\downarrow} \tag{1}$$

with $n_{i,\sigma}=c^{\dagger}_{i,\sigma}c_{i,\sigma}$. $\langle i,j\rangle$ are nearest neighbors on a honeycomb lattice. We denote the total number of sites by $N$ and the number of electrons with a spin projection $\sigma=\uparrow,\downarrow$ by $N_{\sigma}$.

Due to the exponential growth of the Hilbert space dimension with $N$, a direct exact diagonalization of the Hubbard model (1) at half-filling is only possible for system sizes until about 20 sites. In order to deal with larger system sizes we use a MF approximation,

$$H^{MF} = -t \sum_{\langle i,j\rangle,\sigma} c^{\dagger}_{i,\sigma} c_{j,\sigma} + U \sum_{i} (\langle n_{i,\uparrow}\rangle n_{i,\downarrow} + n_{i,\uparrow}\langle n_{i,\downarrow}\rangle - \langle n_{i,\uparrow}\rangle\langle n_{i,\downarrow}\rangle). \tag{2}$$

It should be noted that the MF approximation breaks the SU(2)-symmetry of the original Hubbard model (1).

We compute the ground state

$$|GS\rangle = \prod_{\alpha\le N_{\uparrow}} d^{\dagger}_{\uparrow\alpha} \prod_{\beta\le N_{\downarrow}} d^{\dagger}_{\downarrow\beta} |0\rangle, \quad d_{\sigma,\alpha} = \sum_{i} Q^{*}_{\sigma,\alpha i} c_{\sigma,i} \tag{3}$$

and the one-electron spectrum $\epsilon_{\sigma,\alpha}$ of the MF Hamiltonian (2) using the LAPACK library.

This yields the ground-state energy, the local density

$$\langle n_{\sigma,i}\rangle = \sum_{\alpha\le N_{\sigma}} Q^{*}_{\sigma,\alpha i} Q_{\sigma,i\alpha}, \tag{4}$$

the local magnetization $\langle S^{z}_{i}\rangle=\frac{1}{2}\langle n_{i,\uparrow}-n_{i,\downarrow}\rangle$, as well as the spin correlation functions

 

$$\langle S_i^z S_j^z \rangle = \frac{1}{4}\Bigg( \sum_{\sigma=\uparrow,\downarrow} \sum_{\alpha=1}^{N_\sigma} \sum_{\beta\neq\alpha}^{N_\sigma} Q_{\sigma,j\alpha} Q_{\sigma,i\beta} \times \{ Q^*_{\sigma,\alpha j} Q^*_{\sigma,\beta i} - Q^*_{\sigma,\beta j} Q^*_{\sigma,\alpha i} \} - \langle n_{j\uparrow}\rangle\langle n_{i\downarrow}\rangle - \langle n_{j\downarrow}\rangle\langle n_{i\uparrow}\rangle \Bigg)$$

$$\langle S_i^x S_j^x \rangle = \langle S_i^y S_j^y \rangle = -\frac{1}{4}\Bigg( \sum_{\alpha=1}^{N_\uparrow} \sum_{\beta=1}^{N_\downarrow} Q_{\uparrow,j\alpha} Q_{\downarrow,i\beta} Q^*_{\downarrow,\beta j} Q^*_{\uparrow,\alpha i} + Q_{\uparrow,i\alpha} Q_{\downarrow,j\beta} Q^*_{\downarrow,\beta i} Q^*_{\uparrow,\alpha j} \Bigg) \tag{5}$$

for $i \neq j$ and

$$\langle S_i^z S_j^z \rangle = \langle S_i^x S_j^x \rangle = \langle S_i^y S_j^y \rangle = \frac{1}{4}(\langle n_{i\uparrow}\rangle + \langle n_{i\downarrow}\rangle - 2\langle n_{i\uparrow}\rangle\langle n_{i\downarrow}\rangle) \tag{6}$$

for $i=j$.

Self-consistency requires that the expectation values $\langle n_{\sigma,i}\rangle$ entering (2) are equal to the expression (4) derived from this Hamiltonian. We solve this condition iteratively using suitable initial conditions with given numbers of electrons $N_\sigma$. To overcome convergence problems, we use a thermal state compatible with the Fermi-Dirac distribution at a given temperature instead of the ground state for the first iterations.[22] In this case the average density is computed as

$$\langle n_{\sigma,i}\rangle = \sum_{\alpha\in\Omega_\sigma} Q^*_{\sigma,\alpha i} Q_{\sigma,i\alpha},$$

where $\Omega_\sigma$ is a set of $N_\sigma$ single-particle states chosen randomly with probability $n(\epsilon_{\sigma,\alpha}) = 1/(1+e^{[\beta(\epsilon_{\sigma,\alpha}-\bar{\epsilon})]})$.

## III. RESULTS OF THE MEAN-FIELD APPROXIMATION

### A. System with periodic boundary conditions

First we briefly discuss the MFT for the infinite system with periodic boundary conditions. If we assume a Néel-ordered configuration, we find a Mott-Hubbard phase transition at the literature value $U_c \approx 2.23t$,[21] where the system goes from a paramagnetic semimetal to an insulator with antiferromagnetic order. The asymptotic behavior of the Néel order parameter and the single-particle gap is numerically consistent with linear behavior in $U-U_c$ for $U>U_c$, i.e., associated critical exponents equal to one. These unusual mean-field exponents reflect the unusual density of states[21] which is linear close to the Fermi energy (compare also Ref. 23).

We use the critical value $U_c$ mainly to choose an approximate value of $U$ to describe graphene. In fact, the correct value of the Coulomb interaction in graphene is not yet known. Taking the value of $U$ in polyacetylene, where $U=10$ eV and $t=2.5$ eV, suggests $U \approx 4t$ for graphene.[2] Since, at the MF level, this value locates the system well inside the antiferromagnetic phase and it is observed that large graphene sheets do not show magnetic order, we have decided to use a value of $U$ smaller than $U_c$, $U=2t$ for the following computation.

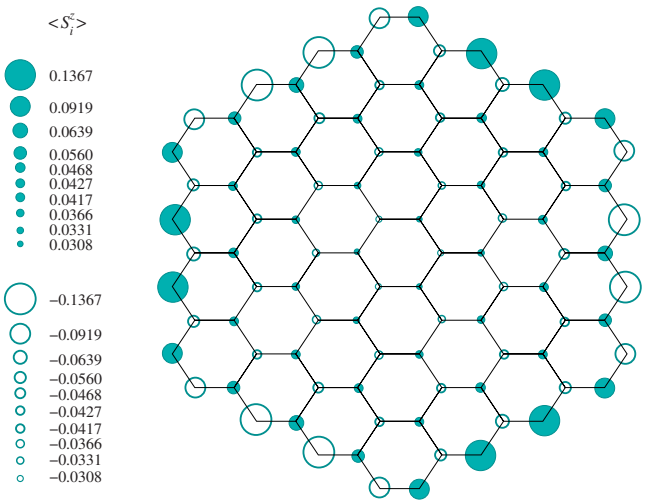


FIG. 1. (Color online) Mean-field result for the edge magnetization of a hexagonal graphene quantum dot with $N=96$ sites and zigzag edges (at half-filling and with $U=2t$).

### B. Edge magnetism on zigzag edge

It is well known that even for values of $U$ smaller than the critical value $U_c$, one observes a form of ferromagnetism on the zigzag edge of a graphene ribbon[9,13,16,17] or a quantum dot.[14,15,19] As an example, Fig. 1 shows our results for the local magnetization of a hexagonal dot with 96 sites. One observes local ferromagnetic behavior at each zigzag edge. By contrast, systems with armchair edges do not show specific magnetic properties and follow an evolution closer to the one of a system with periodic boundary conditions. The difference between the two edges appears to be a consequence of the fact that in the zigzag case only one sublattice is represented on the edge while in the armchair case both sublattices are present. Detailed explorations[15,17] demonstrated that the ferromagnetism of zigzag edges resists to armchair defects and appears already for short edges.

## IV. ACCURACY OF THE APPROXIMATION

### A. Comparison with exact diagonalization for open boundary conditions

To verify the accuracy of the MFT we first compare the results with those obtained with exact diagonalization (ED) of the Hubbard model which was performed with Spinpack.[24] Due to the exponential growth of the Hilbert space, ED is limited to very small systems. Here we have studied the dotlike cluster of 16 sites shown in the inset of the top panel of Fig. 2. The following quantities were computed: (i) the ground-state energy. (ii) The charge gap defined as $\Delta E = E_{N-1} - 2E_N + E_{N+1}$, where $E_n$ is the ground-state energy in the sector with $n$ electrons. Within MFT the charge gap can be identified with the single-particle gap $\Delta_{sp}$. (iii) The $z$- and total staggered magnetization as defined in terms

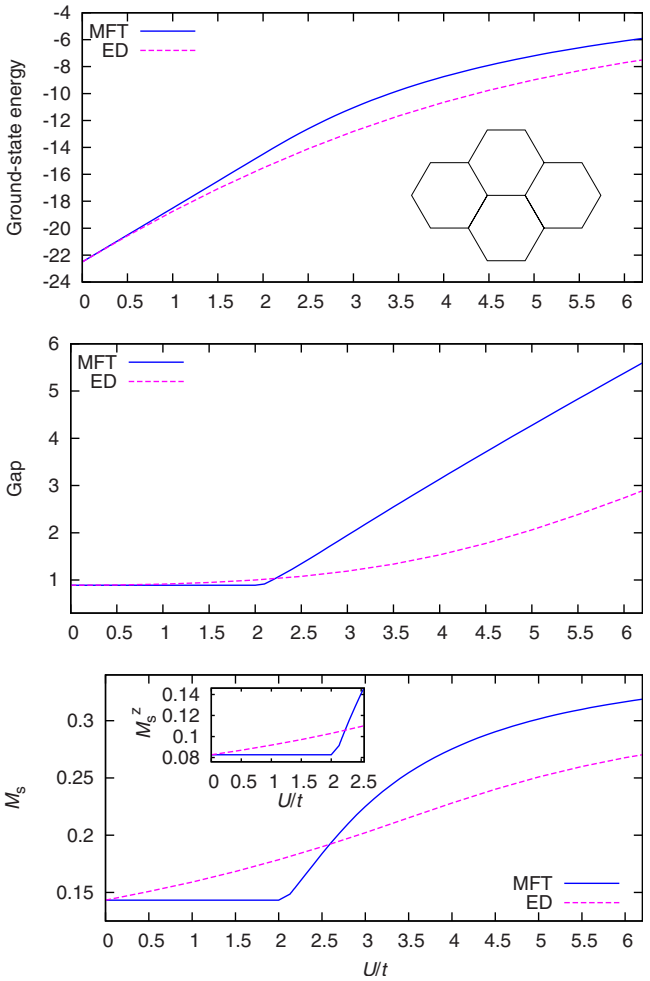


FIG. 2. (Color online) Comparison MFT-ED for the finite-size system of 16 sites sketched in the inset of the top panel at half-filling. The bottom panel shows the total staggered magnetization $M_s$ in the main panel and the $z$-component $M_s^z$ in the inset.

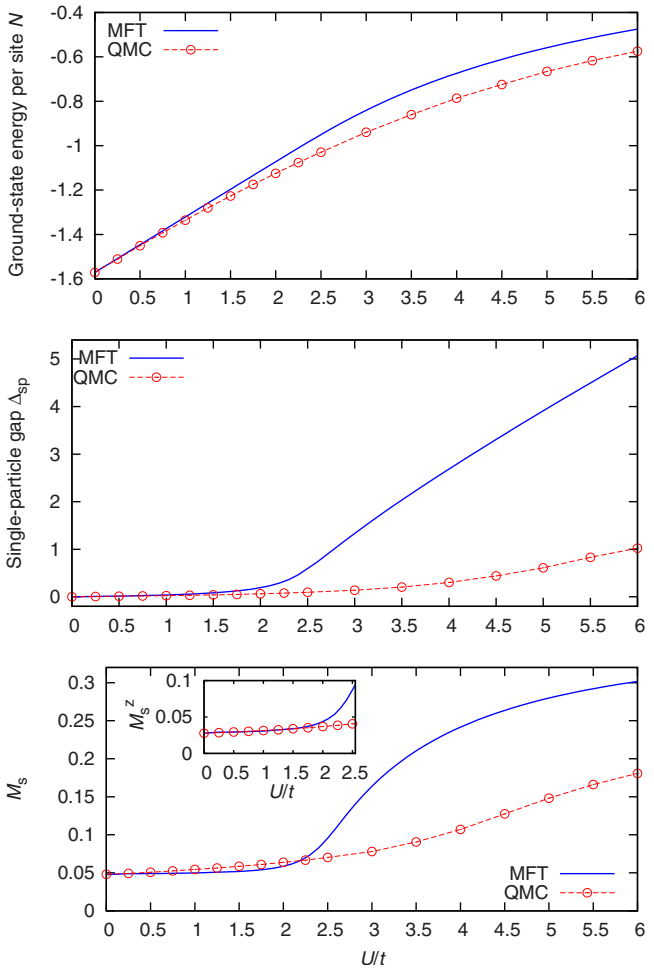


FIG. 3. (Color online) Comparison MFT-QMC for a system with periodic boundary conditions and $N=162$ sites at half-filling. QMC error bars are smaller than the size of the symbols.

of the longitudinal and total spin structure factor

$$M_s^z = \frac{1}{N}\sqrt{\sum_{i,j}(-1)^{i-j}\langle S_i^z S_j^z\rangle}, \tag{7}$$

$$M_s = \frac{1}{N}\sqrt{\sum_{i,j}(-1)^{i-j}\langle \vec{S}_i \cdot \vec{S}_j\rangle}. \tag{8}$$

Here, $(-1)^{i-j}$ is a short-hand notation for $+1$ $(-1)$ if $i$ and $j$ belong to the same (different) sublattice(s). Within MFT, the correlation functions appearing in Eqs. (7) and (8) are computed from Eqs. (5) and (6). In a numerical solution of the Hubbard model respecting SU(2) symmetry one finds $M_s^z = M_s/\sqrt{3}$.

Figure 2 shows a comparison of ground-state energy, charge gap, and the two staggered magnetizations computed both with MFT and ED at half filling, i.e., a total of 16 electrons. As expected, the two methods yield identical results for $U=0$ and the MF ground-state energy is always above the exact answer. The results for all three quantities stay close for $U \lesssim 2t$. This supports the applicability of MFT at least as a semiquantitative method in particular for the parameters of the dot shown in Fig. 1.

### B. Comparison to quantum Monte Carlo for periodic boundary conditions

In order to assess the quality of the MFT for larger but still finite systems, we employ QMC simulations. We use a projective determinantal QMC approach[25] to obtain ground-state properties at half-filling. Within this scheme, expectation values of a physical observable $A$ are obtained from

$$\langle A\rangle = \lim_{\Theta\to\infty}\frac{\langle \Psi_T|e^{-\Theta H/2}Ae^{-\Theta H/2}|\Psi_T\rangle}{\langle \Psi_T|e^{-\Theta H}|\Psi_T\rangle}, \tag{9}$$

where the trial wave function $|\Psi_T\rangle$ must be nonorthogonal to the ground state and $\Theta$ corresponds to a projection parameter. We found $\Theta = 40/t$ to be sufficient to obtain converged ground-state quantities within the statistical uncertainty. For the presented simulations, $\Theta$ was split into discrete step $\Delta\tau$ in the Trotter decomposition. We verified by extrapolating $\Delta\tau \to 0$ that taking $\Delta\tau = 0.05/t$ produced no discretization ar-

tifacts. The simulations were performed on systems with periodic boundary conditions.

Figure 3 shows our QMC and MFT data for a finite system with $N=162$ lattice sites. The top panel of Fig. 3 shows the energy per site. In the middle panel of Fig. 3 we compare the single-particle gap $\Delta_{sp}$ between MFT and QMC. In the QMC simulations $\Delta_{sp}(\vec{k})$ was obtained by fitting the exponential tail of the imaginary-time displaced Green's function $G(\vec{k},\tau) \propto \exp[-\tau\Delta_{sp}(\vec{k})]$ at large imaginary time $\tau$. The single-particle gap $\Delta_{sp}$ shown in Fig. 3 equals $\Delta_{sp}(K)$, i.e., the smallest excitation gap at the Dirac points. Finally, the bottom panel of Fig. 3 compares the QMC results for the total staggered magnetization Eq. (8) (main panel) and the $z$-component Eq. (7) (inset) with the MFT results.

Again, the MFT follows the QMC results closely for $U \lesssim 2t$. In the present case, the MF curves for the energy, single-particle gap $\Delta_{sp}$, and $M_s^z$ are always above the QMC curves. In fact, one observes that in the regime $U \lesssim 2t$ the agreement between MFT and QMC is a bit better for $M_s^z$ than for $M_s$. This can be attributed to the MF approximation explicitly breaking the SU(2) symmetry. Indeed, in this case one finds that the MF contribution of the $x$ and $y$ components to $M_s$ are independent of $U$ for $U>0$ whereas the $z$ component increases with increasing $U$.

Appreciable quantitative differences can be observed in Fig. 3 at large $U$ in particular in $\Delta_{sp}$ and $M_s$. Indeed, MFT is known to underestimate the stability-range of the paramagnetic semimetal by about a factor 2,[21,26] i.e., quantitative differences are expected for $U$ larger than the mean-field critical value $U_c \approx 2.23t$. Furthermore, in the limit $U \to \infty$ we expect to recover the $S=1/2$ Heisenberg model where it is known (compare, e.g., Refs. 27 and 28) that a full quantum mechanical treatment of the quantity defined in Eq. (8) yields a value which for large $N$ is only about 55% of the classical (i.e., MF) value $M_s=1/2$. The difference at the right boundary of the bottom panel of Fig. 3 is indeed of this order. While the MFT and QMC deviate in the precise position of the quantum critical point, they agree on locating the system in the paramagnetic semimetallic phase for $U \leq U_c \approx 2.23t$ and the correspondence is at least semiquantitative for a finite-size system and $U \lesssim 2t$.

## V. CONCLUSION AND PERSPECTIVES

We investigated a self-consistent mean-field approximation to the Hubbard model on the honeycomb lattice, concentrating on half-filling. The infinite system exhibits a Mott-Hubbard transition from a paramagnetic semimetal for a Coulomb repulsion $U<U_c$ to an antiferromagnetic insulator for $U>U_c$ with a MF critical value $U_c \approx 2.23t$.[21] The mean-field critical exponents associated to the gap and Néel order parameter are numerically consistent with the value one.[21]

We studied the accuracy of the MFT for finite-size systems with complementary exact diagonalization and quantum Monte Carlo simulations of the Hubbard model. We computed the ground-state energy, the single-particle gap, and the staggered magnetizations obtained from the spin correlation functions. The MFT reproduces the qualitative behavior found by the other two methods. Furthermore, the quantitative agreement is reasonable for $U \lesssim 2t$, i.e., the region which is identified as a paramagnetic semimetal both by MFT and QMC. For large values of $U$, quantitative differences become appreciable. However, the latter regime corresponds to an antiferromagnetic insulator, not relevant to graphene.

A weak-coupling instability to a canted antiferromagnet emerges in graphene when an in-plane magnetic field is turned on.[29] This weak-coupling instability can be captured at the mean-field level and is confirmed by QMC simulations.[29] Being equally a weak-coupling phenomenon, we believe that it will be possible to observe edge ferromagnetism in future QMC simulations with zigzag boundary conditions. Nevertheless, the MFT has access to bigger systems than QMC since it is numerically less demanding. Here we have presented evidence that the MFT may be expected to be quantitatively reliable for $U \lesssim 2t$.

## ACKNOWLEDGMENTS

We wish to thank T. C. Lang for fruitful discussions, NIC Jülich and HLRS Stuttgart for the allocation of computer time, and the ESF for financial support through the INSTANS program. A.H. acknowledges support by the Deutsche Forschungsgemeinschaft through Grant No. HO 2325/4-1 and S.W. and Z.Y.M. through Grant No. WE 3649/2-1.

[1] K. S. Novoselov, A. K. Geim, S. V. Morozov, D. Jiang, Y. Zhang, S. V. Dubonos, I. V. Grigorieva, and A. A. Firsov, Science **306**, 666 (2004).
[2] A. H. Castro Neto, F. Guinea, N. M. R. Peres, K. S. Novoselov, and A. K. Geim, Rev. Mod. Phys. **81**, 109 (2009).
[3] L. A. Ponomarenko, F. Schedin, M. I. Katsnelson, R. Yang, E. W. Hill, K. S. Novoselov, and A. K. Geim, Science **320**, 356 (2008).
[4] B. Wunsch, T. Stauber, and F. Guinea, Phys. Rev. B **77**, 035316 (2008).
[5] C. Stampfer, J. Güttinger, F. Molitor, D. Graf, T. Ihn, and K. Ensslin, Appl. Phys. Lett. **92**, 012102 (2008).
[6] K. Nakada, M. Fujita, G. Dresselhaus, and M. S. Dresselhaus, Phys. Rev. B **54**, 17954 (1996).
[7] L. Brey and H. A. Fertig, Phys. Rev. B **73**, 235411 (2006).
[8] E. V. Castro, N. M. R. Peres, J. M. B. Lopes dos Santos, A. H. Castro Neto, and F. Guinea, Phys. Rev. Lett. **100**, 026802 (2008).
[9] M. Fujita, K. Wakabayashi, K. Nakada, and K. Kusakabe, J. Phys. Soc. Jpn. **65**, 1920 (1996).
[10] K. Wakabayashi, M. Fujita, H. Ajiki, and M. Sigrist, Phys. Rev. B **59**, 8271 (1999).
[11] T. Hikihara, X. Hu, H.-H. Lin, and C.-Y. Mou, Phys. Rev. B **68**, 035432 (2003).

[12] H. Lee, Y.-W. Son, N. Park, S. Han, and J. Yu, Phys. Rev. B **72**, 174431 (2005).
[13] Y.-W. Son, M. L. Cohen, and S. G. Louie, Phys. Rev. Lett. **97**, 216803 (2006).
[14] J. Fernández-Rossier and J. J. Palacios, Phys. Rev. Lett. **99**, 177204 (2007).
[15] S. Bhowmick and V. B. Shenoy, J. Chem. Phys. **128**, 244717 (2008).
[16] E. V. Castro, N. M. R. Peres, and J. M. B. Lopes Dos Santos, J. Optoelectron. Adv. Mater. **10**, 1716 (2008).
[17] H. Kumazaki and D. S. Hirashima, J. Phys. Soc. Jpn. **77**, 044705 (2008).
[18] J. J. Palacios, J. Fernández-Rossier, and L. Brey, Phys. Rev. B **77**, 195428 (2008).
[19] J. Viana-Gomes, V. M. Pereira, and N. M. R. Peres, Phys. Rev. B **80**, 245436 (2009).
[20] O. V. Yazyev and M. I. Katsnelson, Phys. Rev. Lett. **100**, 047209 (2008).
[21] S. Sorella and E. Tosatti, Europhys. Lett. **19**, 699 (1992).
[22] D. C. Cabra and G. L. Rossini, Phys. Rev. B **69**, 184425 (2004).
[23] I. F. Herbut, V. Juričić, and B. Roy, Phys. Rev. B **79**, 085116 (2009).
[24] J. Schulenburg, http://www-e.uni-magdeburg.de/jschulen/spin/index.html
[25] F. F. Assaad and H. G. Evertz, Lect. Notes Phys. **739**, 277 (2008).
[26] N. Furukawa, J. Phys. Soc. Jpn. **70**, 1483 (2001).
[27] J. Richter, J. Schulenburg, and A. Honecker, Lect. Notes Phys. **645**, 85 (2004).
[28] E. V. Castro, N. M. R. Peres, K. S. D. Beach, and A. W. Sandvik, Phys. Rev. B **73**, 054422 (2006).
[29] M. Bercx, T. C. Lang, and F. F. Assaad, Phys. Rev. B **80**, 045412 (2009).